A Computational Tool for Geometric Characterization of Pores and Fractures in Microtomography Rock Images

Uma Ferramenta Computacional para a Caracterização Geométrica de Poros e Fraturas em Imagens de Microtomografia de Rochas

Letícia da Silva Bomfim[1], Guilherme Daniel Avansi[2], Alexandre Campane Vidal[3] and Helio Pedrini[4]

[1] Institute of Computing, University of Campinas (UNICAMP), Campinas, SP, Brazil, 13083-852. leticiabomfim4@gmail.com
ORCID: https://orcid.org/0000-0002-7675-7937

[2] SOLPE - Oil Reservoir Solutions, Campinas, SP, Brazil, 13083-898. guiavansi@gmail.com
ORCID: https://orcid.org/0000-0003-1720-5080

[3] Institute of Geosciences, University of Campinas (UNICAMP), Campinas, SP, Brazil, 13083-855. vidal@unicamp.br
ORCID: https://orcid.org/0000-0002-9613-1261

[4] Institute of Computing, University of Campinas (UNICAMP), Campinas, SP, Brazil, 13083-852. helio@ic.unicamp.br
ORCID: https://orcid.org/0000-0003-0125-630X

Abstract: Pores and fractures are key structures that allow for the propagation and conduction of fluids and chemical substances inside reservoirs. The interconnected nature of these spaces facilitates the flow of fluids. To better understand these structures, we have developed a computational tool that utilizes high-resolution images from computed microtomography. This tool aims to detect and characterize the geometry of pores and faults with the goal of providing a detailed understanding of these structures. The tool employs image processing techniques to identify the contours' structure obtained through data segmentation and to evaluate their geometric parameters in conjunction with the algorithms implemented in this work. The purpose of this tool is to reduce the uncertainties found in manual work, prioritize the preservation of important samples collected in the field, and provide assistance in the characterization of reservoirs and fluid analysis.

Keywords: Carbonate Rocks. Fractures. Pores. Image Processing.

Resumo: Poros e fraturas são estruturas cruciais que permitem a propagação e condução de fluidos e substâncias químicas dentro de reservatórios. A natureza interconectada desses espaços facilita o fluxo de fluidos. Para compreender melhor essas estruturas, uma ferramenta computacional foi desenvolvida que utiliza imagens de alta resolução obtidas por microtomografia computadorizada. Esta ferramenta tem como objetivo detectar e caracterizar a geometria de poros e falhas, com a finalidade de fornecer uma compreensão detalhada dessas estruturas. A ferramenta emprega técnicas de processamento de imagens para identificar a estrutura dos contornos obtidos por segmentação de dados e avaliar seus parâmetros geométricos em conjunto com os algoritmos implementados neste trabalho. O propósito desta ferramenta é reduzir as incertezas encontradas no trabalho manual, priorizar a preservação de amostras importantes coletadas no campo e fornecer assistência na caracterização de reservatórios e análise de fluidos.

Palavras-chave: Rochas Carbonáticas. Fraturas. Poros. Processamento de Imagens.

1 INTRODUCTION

Carbonate reservoirs are primarily formed through porous and fractured rocks, making the study of these structures of great importance (COUNCIL, 1996). Therefore, a rock environment abundant in these attributes fosters the creation of optimal conditions for the passage and extraction of chemical fluids in the reservoir.

Pores are empty spaces that vary in shape, arrangement, size, and grain composition of the rock. Fractures are flat surfaces that represent planes of weakness and are caused by partial loss of cohesiveness in the rock due to stress (SINGHAL; GUPTA, 2010). Their existence can either facilitate or impede fluid flow between them. The stress-dependent fracture permeability reported by Li et al. (2021) has significant implications for oil and gas production, underground CO_2 storage, and deep waste disposal containment.

Accurately determining the geometry of both porous and fractured structures is crucial for understanding oil and gas reservoir profiles. This information is essential for feeding flow simulators that utilize mathematical models in porous media to describe mass and/or energy flow based on macroscopic parameters. The impact of the geometric properties of stochastic fracture networks, such as fracture lengths, orientations, openings, and center positions, was investigated by Zhu et al. (2021). Their findings demonstrate the significant implications of these parameters on the main macroscale flow properties.

To analyze the macroscale parameters of reservoirs, geological materials must be collected from them. However, the collection process is arduous and costly, and the sample's integrity is often at risk. To preserve and perpetuate the collected material, there has been widespread encouragement for the development and application of non-destructive methods for its analysis.

The application of digital non-destructive methods is crucial because manual analysis of geological samples to obtain their properties is challenging. Jing and Stephansson (2007) noted that comprehensively investigating all individual fractures to create a deterministic model for analysis or design is impractical due to the vast number of fractures in this medium, as well as their varied distributions.

The computerized microtomography technique presents an excellent opportunity for this task. Unlike laboratory experiments, this approach avoids modifying the permo-porous characteristics of the sample, preserving its durability and integrity, while providing deeper visualization than manual study allows. Additionally, this technique facilitates the application of image analysis to the acquired images. It is important to note that microtomography does not aim to replace laboratory experiments, but rather to complement them. As illustrated in Figure 1, the technique enables the observation of the two main structures of interest in carbonate rocks, pores and fractures.

Figure 1 – Microtomography image of carbonate rock containing both pores and a fracture.
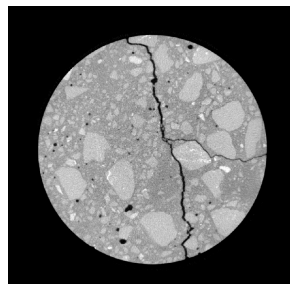
Source: (PLASIS, 2014).

Given these factors, we utilized microtomography images due to their high resolution to identify and characterize pores and fractures present in rocks. We developed a method that operates in two dimensions (2D) by segmenting and extracting the structures from the set of tomographic images generated from a sample. This approach enabled us to analyze the detected components and present their parameters.

The tool not only analyzes each structure individually but also conducts a global scale analysis of the 2D sample being processed. This involves analyzing the data of the complete set of fractures and pores found to quantify their number, density, porosity, and geomorphological characteristics.

This paper is an extended version of the work previously developed by Bomfim and Pedrini (2022), presented at the XXIII Brazilian Symposium on GeoInformatics (GeoInfo 2022), which described a fracture geometry characterization method from computed microtomography rock images.

The text is structured as follows. Section 2 provides a theoretical framework that presents relevant concepts regarding the characteristics to be extracted from fractures and pores. Section 3 presents the materials used in this research, starting from the presentation of the database to the computational tools used. Section 4 describes the methodology and the graphical tool interface that were developed. Section 5 presents and discusses the experimental results obtained. Finally, Section 6 describes the conclusions drawn from this work and provides directions for future research.

2   BACKGROUND

This section starts with an overview of recent research on rock analysis using computed microtomography. Then, we describe the pores and faults characteristics that will be evaluated in the experiments.

2.1   Related Work

The study of fluid flow often involves the analysis of carbonate rocks due to their properties (SANTOS et al., 2022). Pores and fractures, the main components of carbonate rocks, can provide important insights into reservoir exploration. Non-wetting fluid injection has been a traditional and precise method for analyzing this material, with helium gas expansion being the most accurate method, as indicated by Lucia et al. (2003). Al Shafloot et al. (2021) and Yang et al. (2021) have investigated fracturing behavior and propagation using non-wetting fluids such as carbon dioxide and nitrogen, and have continuously monitored in situ details using X-ray Computed Tomography (CT). Utilizing this technology for monitoring fracture propagation and characteristics has provided valuable insights into the visualization capabilities offered by MicroCT. Despite encountering challenges related to image quality, it has demonstrated excellent performance in these activities.

A study conducted by Basan et al. (1997) on core material analyzed the data using three different techniques: capillary mercury injection pressure (MICP), backscattered electron imaging (BSEI), and nuclear magnetic resonance (NMR). The authors found that the data provided by these three techniques were suitable for cross-correlation analysis to obtain a visual and quantitative analysis of the pore structure. They further stated that NMR techniques have the potential to not only improve reservoir simulations but also provide crucial insights into the factors regulating reservoir performance.

Several studies have utilized X-ray techniques to acquire data and study rock samples in detail, taking advantage of the high resolution and visualization capabilities of computed microtomography. Cnudde and Boon (2013) highlighted the importance of computed microtomography in geosciences due to recent technological advancements and computational progress. For instance, Macdonald et al. (2022) used microtomography to capture models of complex geometry, enabling the measurement and characterization of lithic tools and the mathematical calculation of edge curvature. This groundbreaking archaeological study presented the first investigation focusing on the measurement of overhang features.

Dong et al. (2008) and Sok et al. (2010) investigated the pore networks formed in these samples by microtomography images, with the purpose of developing a more accurate model to comprehend the behavior of fluid flow. In their work, Dong et al. conducted a comparative analysis of four different methods in the literature for extracting pore skeletons in 3D, among them, the maximal ball methods (denoted MB) that identifies the largest inscribed spheres at each voxel in the pore space, and the flow velocity-based method (denoted VB) that generates a pore skeleton, demonstrated superior performance in extracting accurate results. On the other hand, Sok et al. analyzed the different relationships between the scales provided by various image acquisition methods (such as MicroCT, scanning electron microscopy (SEM), and focused ion beam SEM) and rock samples. They examined the quality of information extracted by comparing it with the real scale, leading to the identification of a method that exhibits better correspondence based on the scale of the actual sample.

Xiong et al. (2021) employed image processing techniques to propose a method for analyzing fracture characteristics, specifically focusing on the extraction of three-dimensional fracture networks to investigate preferential fluid migration paths. Notably, this method introduced a new approach to rock flow analysis, surpassing the commonly used finite volume analysis (FVM) method in terms of computational efficiency. Li et al. (2022) utilized a three-dimensional reconstruction to study how fractures propagate and interact. They employed several procedures such as stacking, recording, and segmentation of successive images of serial cuts, resulting in a 3D fracture model in the form of a valuable dataset that enables not only the investigation of hydraulic fracturing mechanisms, but also for fracture aperture quantification and evaluation of fluid transmissivity.

Segmentation is a critical step in image processing for extracting information from data (PEDRINI, 2001; PEDRINI; SCHWARTZ, 2007; SCHWARTZ; PEDRINI, 2006). Deng et al. (2016) developed an interactive local thresholding technique to segment fractures and rock grains, significantly increasing the number of classes in the gray scale. This enabled them to study the permeability caused by the fractures. Similarly, Moraes (2018) used the watershed method for segmentation to calculate porosity by separating voxels into two groups: pores and non-pores, making it possible to determine the porosity, permeability and anisotropy of permeability in a digital way, being as accurate as the laboratory approach, and still with the benefit of not destroying the samples.

Purswani et al. (2020) conducted an evaluation of segmentation methods using two machine learning approaches: supervised and unsupervised (Fast Random Forest versus K-means combined with fuzzy logic), and compared them with traditional thresholding methods. Although the supervised approach performed the best, it required a large annotated dataset. Therefore, to avoid this limitation and considering the small difference between the best and traditional models, we opted for using the proven and excellent performing thresholding methods featured in their work, and better described in the next section.

Tang et al. (2017) studied the impact of fracture network formation by analyzing the effects of connectivity and fracture length on the electrical formation factor, using percolation theory. In their research, a formation factor model was proposed based on a normalized "universal" scaling relation. This model is applicable to fracture networks with constant fracture length and length distributions, highlighting the independence of the normalized scaling law from fracture patterns.

Finally, three notable works emerge in the field of computational tools that aim to characterize structures found in rocks. Hardebol and Bertotti (2013) introduced DigiFract, a software written in Python that utilizes digital photographs of fracture outcrops to support field acquisition based on geographic information system (GIS) technology. Healy et al. (2017) created FracPaQ, a tool implemented in MATLAB that quantifies fracture patterns in digital images, including micrographs, geological maps, outcrop photographs, and aerial or satellite images. In contrast, Ramandi et al. (2022) developed an algorithm called FracDetect that automates the detection of fractures in grayscale 3D microtomography images. These tools also serve as a valuable reference for the development of software with geological applications in the field of geographic information extraction.

The relevance of tools that enable the extraction and analysis of mechanical and transport properties, such as strength, anisotropy, fluids, and heat, has been highlighted in the literature. The adoption of non-destructive techniques for image analysis has played a significant role in identifying key features that aid in extracting these properties from rock samples, leading to a better understanding of the study area. In light of this, we have developed a methodology and a tool that operate within a single environment, aimed at processing and analyzing computed microtomography images.

2.2　Related Concepts

Given the multidisciplinary nature of the research, this section will be organized into two parts: technical concepts, where we will detail some of the computational approaches used, and geological concepts, where we will address the two main structures analyzed in our research, namely, pores and fractures. We will draw on the characteristics described in the literature for their application in image analysis.

2.2.1   Technical Concepts

The process of image segmentation involves dividing an image into objects or regions. Algorithms for image segmentation generally utilize fundamental properties of images, such as abrupt changes in intensity values (such as edges) or the separation of similar regions, such as through thresholding, region growth, or division/merging techniques (GONZALEZ; WOODS, 2007).

The previously mentioned algorithms have different objectives and methodologies. Thresholding, for instance, is a technique that divides an input image $f(x, y)$ of N grayscale levels into a thresholded image with a grayscale level lower than N. In simple cases, N is 2, resulting in two classes labeled as background and object, separated by a threshold T.

An alternative approach to segmenting images using thresholds automatically is to use algorithms such as the method developed by Otsu (1979). This technique aims to maximize the variance between classes by identifying an optimal threshold that provides the best separation between them based on their intensity values.

Mathematical morphology is a field based on set theory that provides another technique for image segmentation called watershed segmentation. This method considers the image as a topographic relief where the pixel value h represents its elevation, and it is used to separate regions. The watershed transform divides the image into "watersheds" that are associated with local minimums. This is typically done by applying a gradient function to partition the image into significant regions, where transitions between regions are defined, such that homogeneous regions will have minimums and edges will have maximums(BEUCHER; MEYER, 2018; GONZALEZ; WOODS, 2007).

On the other hand, if the objective of segmentation is to specifically detect edges, the concept of gradient can also be applied to identify the intensity and direction of the edges in the image. Thus, a derivative operator that is sensitive to changes presented by the gradient will indicate when encountering a sudden variation in the intensity values of the image.

2.2.2   Geological Concepts

This section provides a brief overview of the characteristics of the two main structures inside the rock that were analyzed.

2.2.2.1   Pores

The quantification of porosity is a crucial characteristic to be analyzed in pores. According to Anselmetti et al. (1998), porosity is a significant parameter for the characterization of rocks, providing valuable information about their petrography and physical properties. Porosity is typically defined as the ratio of the volume of empty pores to the total volume of the rock reservoir.

The estimation of rock porosity can be quantitatively determined by analyzing the number of pixels that comprise the pore area and the total area of the image representing the rock (pore and rock combined). The total porosity can be defined as:

$$Porosity = \frac{pore\ volume}{total\ rock\ volume} \tag{1}$$

The calculation of porosity is crucial for the oil industry as it directly impacts the profitability of a reservoir. A reservoir with good productivity is one that not only has large volumes of oil but also favorable conditions for fluid flow (permeability), which leads to successful recovery of fluids and economic viability.

One easily extractable feature of the pore body is its circularity, which can provide insights into the relationship between pore size and shape. Pores with larger diameters are more effective in accumulating and transmitting fluids within the rock. Circularity is measured on a scale of 0 to 1, where a higher value indicates greater circularity. It is calculated using the following equation:

$$circularity = \frac{4\pi\ area}{perimeter^2} \tag{2}$$

Another feature to be analyzed about pores is their visibility, which was classified by Archie (1952) into four categories:

- Class A: not visible, with pores smaller than 1 micrometer.

- Class B: visible, with pores between 1 and 10 micrometers.

- Class C: visible, with pores larger than 10 micrometers.

- Class D: *vugs*, with pores larger than 1 millimeter.

Archie (1952) considered the visibility of pores as crucial in fluid distribution within reservoirs and classified the frequency of visible pores into the categories listed in Table 1.

Table 1 – Categorizing the frequency of visible pores for fluid distribution in reservoirs.

| Description	Frequency - Percentage of Surface Covered by Pores
Excellent	20
Good	15
Fair	10
Poor	5

2.2.2.2 Fractures

According to the National Research Council (COUNCIL, 1996), identifying and locating hydraulically significant fractures is crucial for understanding and predicting fracture behavior. This is because determining their geometry is essential in creating flow simulations, which use mathematical models to describe mass and/or energy flow based on macroscopic parameters (ERTEKIN; ABOU-KASSEM; KING, 2001).

We have identified several indicators to classify a sample containing fractures, including individual characteristics of this structure that can be analyzed, such as:

- The number of fractures identified in the image.

- The size of the fractures, which is a measure of the extent of development of the discontinuity surface. This carries the notion of size and controls the degree of fracturing.

- One of the characteristics of fractures that can be analyzed is the type of connectivity, which refers to how fractures intersect and terminate. Ortega and Marrett (2000) emphasized that connectivity is a fundamental property when it comes to fluid flow. Quantifying this parameter enables the comparison of different fracture networks and facilitates more realistic modeling of fluid flow through fracture systems. Connectivity can be classified into three types, as illustrated in Figure 2, based on the number of fracture connections as follows:

  - Type I: not connected.
  - Type II: individually connected.
 - Type III: multiple connected.

Singhal and Gupta (2010) classified fractures into two types based on their characteristics: systematic and non-systematic fractures. Systematic fractures are planar and have a more regular distribution, whereas non-systematic fractures are irregular and curved. Figure 3 illustrates these two types of fractures.

Figure 2 – Fracture termination types. Isolated fractures (Type I, e.g., *b* fracture), individually connected fractures (Type II, *b* fracture), and fractures connected with other fractures in more than one location (Type III, *b* and *b′* fractures).
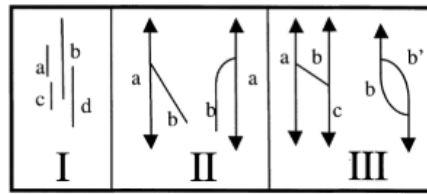
Source: (ORTEGA; MARRETT, 2000).

Figure 3 – Representation of fracture types. (a) systematic and (b) non-systematic.
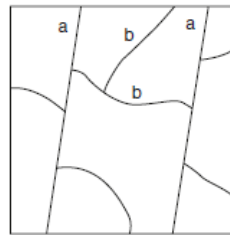
Source: (SINGHAL; GUPTA, 2010).

- The fracture orientation, which can be classified into vertical, horizontal and inclined. This feature generally restricts the potential directions in which fluids can flow in a fractured rock system (INTERSTATE TECHNOLOGY AND REGULATORY COUNCIL (ITRC), 2020).

- The fracture density that corresponds to the degree/intensity of fracturing of the rock, which can be described in three ways: linear, regional and volumetric.

  – Linear fracture density is the average number of fractures in a given set, measured in a direction perpendicular to the fracture plane.

  – Regional fracture density (2D fracture density) is a way to quantify the persistence of discontinuity. It refers to the average length of strokes per unit area on a flat surface.

  – Volumetric fracture density (3D fracture density) is the average fractured surface area per unit rock volume created by all fractures in a given set.

3   MATERIAL

This section describes the datasets utilized in the study and the hardware and software resources employed for the development of the tool.

3.1   Databases

The majority of microtomography images are saved in RAW, TIFF (Tagged Image File Format), or DICOM (Digital Imaging and Communications in Medicine) formats. For this research, grayscale images in TIFF format were utilized, enabling the two-dimensional exploration of the sample slices. TIFF format supports various image sizes and resolutions, as well as color depths, and includes a lossless compression algorithm that preserves details (WIGGINS et al., 2001).

The Digital Rocks Portal (BULTREYS, 2016) is an online repository that facilitates the retrieval, storage, sharing, organization, and analysis of images of distributed porous microstructures. Its objective is to improve research resources for modeling and predicting properties of porous materials in the fields of Petroleum, Civil and Environmental Engineering, as well as Geology.

We obtained sets of images from the Digital Rocks Portal to evaluate the algorithms implemented in our tool. Two databases were primarily used, one of which was the *Sample of Naturally Fractured Coal* (PLASIS, 2014), used to study fractures. This database consists of an image of a coal sample with dimensions of 1634×1634×4115 voxels, and a resolution of 25μm (voxel size and point size).

The second dataset, called the *Estaillades Carbonate #2* (BULTREYS, 2016), was used to study pores. It consists of a monomineral calcite rock sample with a diameter of 7mm, generating a series of images with dimensions 200×2000 pixels. This sample has a porosity of approximately 25% and contains both intergranular macropores and intragranular micropores, allowing for testing with varying pore geometries (BULTREYS et al., 2016).

We have chosen a selection of images from these databases that represent the heterogeneity of the samples, in order to evaluate the tool developed.

3.2 Computational Tools

We employed the Python programming language for the implementation of this project, as it provides various resources in libraries for image manipulation, numerical calculations and graphics display. Some of the notable libraries are:

- NumPy and SciPy for data manipulation. SciPy is a Python ecosystem that is open-source software for mathematics, science, and engineering. It provides many numerical routines that are efficient and user-friendly, such as functions for numerical integration, interpolation, optimization, linear algebra, and statistics. It also uses the Numpy library as its scientific computing base to handle a variety of numeric types (VIRTANEN et al., 2020).

- Scikit-Image and OpenCV are used for image manipulation. Scikit-Image (VAN DER WALT et al., 2014) is an image processing library that implements algorithms and utilities for use in research, education, and industry applications. It enabled us to apply edge detection and segmentation algorithms. On the other hand, OpenCV (OPENCV, 2015) provides a common infrastructure for computer vision applications, and it is best suited for detecting structures segmented by the `findContours()` function. It allows obtaining location, size, and other parameters related to the object.

- Visualization Toolkit (VTK) for 3D visualization. A free and open-source tool that offers a range of features for 3D computer graphics, geometric modeling, graph display, image processing, volumetric rendering, and scientific visualization.

- PyQt and Qt Designer for interface creation. PyQt is a set of Python bindings for the Qt application development framework, which allows developers to create applications that can run on different platforms. Qt Designer is a visual editor for designing dialogs and windows in Qt applications. With this tool, developers can create user interfaces interactively and visually, without writing code.

4 METHODOLOGY

This section outlines the methodology used to apply the fracture and pore detection methods, which were developed for this project. These methods were tested on publicly available databases as previously mentioned, and their application is described in detail.

4.1 Segmentation Process

The process of segmentation is crucial for estimating various properties of pore-scale, such as porosity, fluid saturation, and pore connectivity (PURSWANI et al., 2020). Segmentation of the images is achieved by two steps, which are iteratively executed until the final result is obtained. Firstly, a mask indicating the region of interest in the image is created, followed by the generation of an image denoting the rock content. By combining

the results of both steps, an image containing only the internal structures is obtained for further analysis. The segmentation mask is created by employing a series of image processing techniques that utilize functions from the Scikit-Image and OpenCV libraries.

The process of applying the segmentation algorithms is exemplified in Figure 4. The segmentation begins with the application of Otsu's thresholding (OTSU, 1979) on the original image to extract the best threshold that separates the intensities of the image. Then, a labeled image is created with the object/background regions separated from the obtained threshold, using the following criteria:

$$label(x) = \begin{cases} 1, & \text{if original}(x) < \text{Otsu's thresholding} \\ 2, & \text{if original}(x) \geq \text{Otsu's thresholding} \end{cases} \tag{3}$$

Figure 4 – Diagram that illustrates the segmentation process.
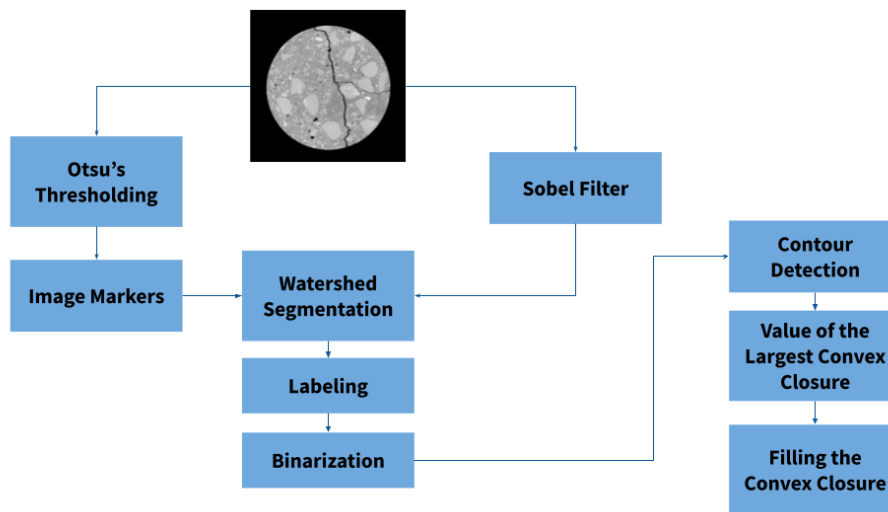
Source: The authors (2023).

To achieve a good segmentation, it is important to generate an elevation map using the Sobel filter, which will be used as a segmentation parameter along with the labeled image. This map is crucial in defining the barriers of image structures, and it allows the application of the watershed technique for the final segmentation.

Once the segmentation process is completed, the labeling technique is applied to the resulting image to assign labels to the segmented regions and create a new binary image model, such that

$$binary(x) = \begin{cases} 0, & \text{if labeling}(x) = 0 \\ 255, & \text{if labeling}(x) \neq 0 \end{cases} \tag{4}$$

The resulting image highlights the region of interest of the image, from which contours are detected. The convex closure analysis is performed on these contours to extract the largest one, which corresponds to the polygon representing the area of the rock. The mask image is then generated by filling the largest convex closure, resulting in a binary output with the white area corresponding to the rock and the black background.

This elaborate segmentation process is crucial because the rock sample typically contains pores or fractures at its edges. A straightforward binarization would make it impossible to count and extract the geometry of these structures since they would not have a clearly defined edge and would be indistinguishable from the background, as seen in the third image of the sequence illustrated in Figure 5. By creating a circular mask that encompasses the entire sample area, all structures within this region of interest can be counted.

The mask created in the previous step is used in combination with another image, which is segmented by Otsu's thresholding, to provide greater accuracy in capturing fractures. The resulting image is a combination of the two, in which white pixels in both the mask and the thresholded image are retained, while black pixels are discarded. This process results in an image that shows only the pores/fractures, as depicted in Figure 5.

9

Figure 5 – Microtomographic image and the resulting segmentation. (a) original image, (b) mask image, (c) image generated by the Otsu's thresholding and (d) image resulting from the two previous ones.
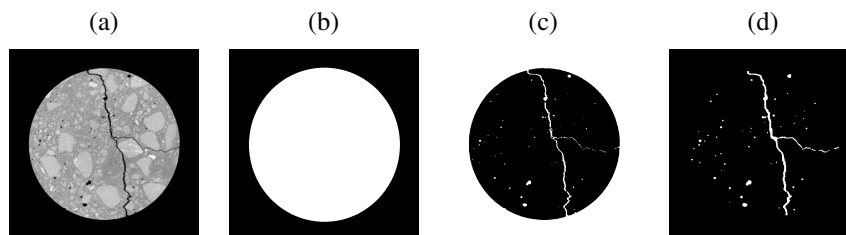
Source: The authors (2023).

4.2   Feature Extraction: Pores

To analyze the features extracted by the pore segmentation, the contour detection was performed using the `findContours()` function. This function returns the parameters required to calculate the circularity value of the pores and analyze their visibility class. The pore area was obtained through the `contourArea()` function, while the `arcLength()` function was used to obtain the pore perimeter, which is necessary to calculate circularity. Additionally, the `minEnclosingCircle()` function was applied to find the pore radius, which provides the smallest circle that encloses the pore boundary.

To calculate the porosity metric, it is necessary to count the number of empty pixels in the slice and the total area of the sample. To do this, we first extract the area relative to the pores by counting the number of white pixels in the final segmentation image, and the total area by counting the white pixels in the mask image. However, we must exclude the area of non-visible pixels from this value, as the absolute porosity is determined by the visible pores.

The information obtained from these functions is stored in data structures in the form of lists, which can be further processed and analyzed using graphs to visualize the behavior of the porous sample.

4.3   Feature Extraction: Fractures

To analyze the characteristics of the segmented image, the contours extracted from the original image need to be identified. The `findContours()` function from the `OpenCV` library is used for this purpose, where the segmented image is passed as a parameter and the identified contours are returned.

Fractures are characterized by an elongated body that resembles a straight line. Therefore, we utilize this criterion to differentiate fractures from other structures such as pores. To identify this feature, we apply the Hough line transform to a subimage extracted from the bounding box of the contour body. If a line can be drawn, we classify this contour as a fracture. Otherwise, it is excluded from subsequent steps. Figure 6 illustrates an example of this process applied to fractures identified in a coal sample.

Figure 6 – Line detection by the Hough line transform.
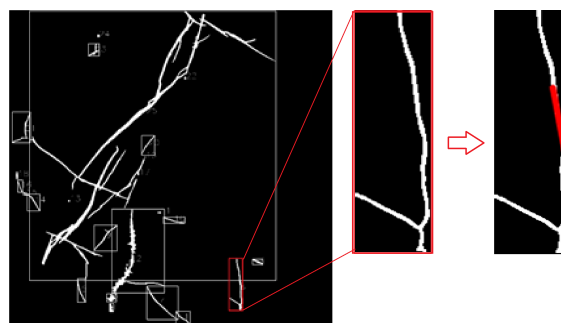
Source: The authors (2023).

After the contour extraction and fracture identification process, the characteristics described in Sub-

section 2.2 are analyzed. The Hough line transform is used not only for fracture identification but also for calculating their slope through the equation of the distance between two points (x_1, y_1) and (x_2, y_2) expressed in degrees. This equation can be written as:

$$angle = \arctan(\frac{y_1 - y_2}{x_1 - x_2}) * \frac{180}{\pi} \tag{5}$$

Obtaining characteristics such as area, height, and width can be achieved through the same function that extracts the contour, as its return includes data about the object's geometry. The density calculation was based on the concepts described in Section 2. It is obtained through the pixels that form the fracture.

The number of fractures by the diameter of the rock sample is used to determine the 1D density, given by:

$$d_1 = \frac{number\ of\ fractures}{diameter} \tag{6}$$

The 2D densitiy is calculated by averaging the width of the fractures by the total area of the sample, expressed as:

$$d_2 = \frac{mean(width\ of\ fractures)}{total\ sample\ area} \tag{7}$$

Finally, the 3D density determined through the ratio of the fracture area to the sample area, expressed as:

$$d_3 = \frac{total\ area\ of\ fractures}{total\ sample\ area} \tag{8}$$

To characterize the fracture structure, a more sophisticated analysis is required due to its unique features. This is mainly due to the fact that many fractures can be in close proximity, making individual analysis difficult. To overcome this, two methodologies were developed to define these criteria:

- Connectivity: involves identifying fracture bifurcations, which requires traversing each column of the non-rotating bounding box of each fracture. This process counts the number of transitions occurring from the intensity relative to the fracture (white) to the background of the image (black). If there are more than one transition on the same line, this indicates that there would be a bifurcation, raising its classification type (Types I, II, III) with each transition found. However, this algorithm produces incorrect results as some fractures have parts of others inserted in their bounding box, as shown in Figure 7. To address this issue, the labeling technique was applied based on the study of some methods for identifying connected components (CC). From this concept, labeling assigns the same label to a CC, making it possible to apply the initial algorithm again, but this time with the structures of a labeled bounding box. The fracture with the largest domain receives a label equal to 1 and the background of the image receives a label 0, allowing transitions to be counted only when they occur between these two values. If there is another fracture in the bounding box, it will receive another label, with the number 2 (shown in blue), not interfering with the result.

Figure 7 – Identification of external components in the bounding box of a fracture.
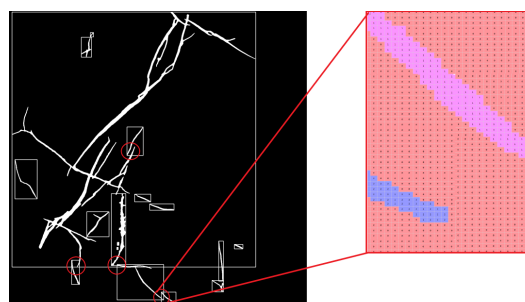
Source: The authors (2023).

- **Type**: to distinguish systematic fractures from non-systematic ones, the thickness of several fracture styles was analyzed. It was observed that systematic fractures, which do not have bifurcations, had a width smaller than 60 pixels. Therefore, this value was adopted as a threshold for this parameter.

4.4 3D Visualization

We implemented a function that enables the visualization of segmented images in 3D using the VTK tool. This function provides a comprehensive view of the distribution of structures of interest.

The `vtkTIFFReader()` class enables VTK to read images in TIFF format. Once the images are read, a transfer function is defined to map a property (scalar value) to an RGB (Red-Green-Blue) color value through the `vtkColorTransferFunction()` class. In addition, opacity is set to only visualize white structures, while the black color of the image is eliminated by adding transparency.

A 3D visualization of the segmented images is created using the `vtkSmartVolumeMapper()` class, which generates a volume mapping in 3D space. This is then added to the rendering screen for display. To provide an interactive experience, an object of the `QVTKRenderWindowInteractor()` class is integrated into the screen. This allows users to change their view of the sample by manipulating the rendered object with their mouse.

5 RESULTS

One way to present the parameters identified in the literature and implemented through the previously described methods is by creating an interactive tool with dedicated sections for analyzing pores and fractures. By using this tool, users can load a set of microtomography images related to a rock sample, or a few images, and analyze them individually or collectively.

The tool allows for conversion of the presented values to the actual scale of the sample by specifying the pixel-millimeter scale used for image acquisition. If the scale is unknown, a default value of 1 can be used, and the results will be presented in pixels.

The fractures section of the tool, as illustrated in Figure 8, displays all the relevant information regarding image loading and the fracture parameters. Upon loading the images, two main screens will display the first image of the set and its segmented version. The `SliceBar` allows the user to interact with the tool by selecting the slice of the image set they wish to view. The tool then automatically updates the displayed information corresponding to the selected image.

Figure 8 – User interface used to analyze and visualize fractures.
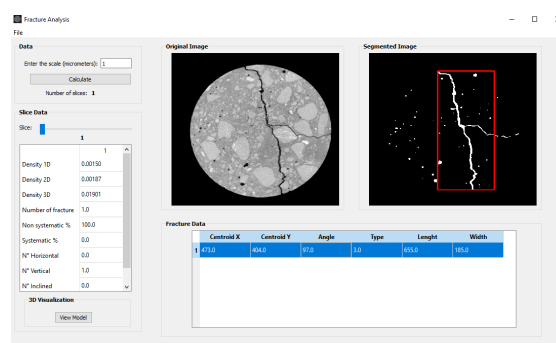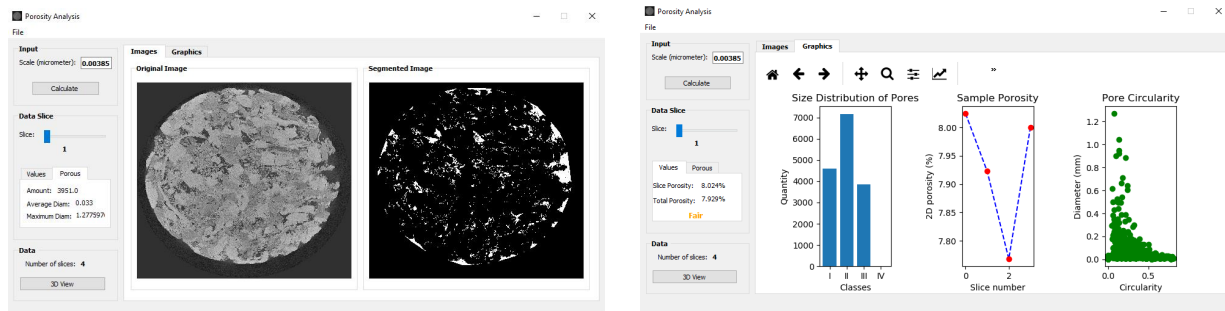

Source: The authors (2023).

Two tables are displayed in addition to the images, showing fracture data. The first table presents the data for the entire slice, displaying the number of fractures, densities (1D, 2D, and 3D), the number of vertical, horizontal, and inclined fractures, and the percentage of systematic and non-systematic fractures. The second table, located below the images, presents the data for each individual fracture, with each row corresponding to a different fracture. To better correlate the numbers with the segmented images, clicking on a row in the table highlights the corresponding fracture in the segmented image.

The section of the tool developed for analyzing pores, as shown in Figure 9, allows the user to interact with the different slices of the input images in a similar way to the fracture analysis section. The `SliceBar` functionality enables the user to switch between slices, with both the original and the segmented image, and the corresponding porosity values being updated accordingly. The total porosity value displayed on the interface is always the same, regardless of the slice being analyzed, as it corresponds to the overall value calculated for the entire sample provided to the tool.

Figure 9 – Interface screen to analyze and visualize pores.

Source: The authors (2023).

Further data is displayed in colored text, indicating the porosity class of the sample (poor: red, fair: orange, good: yellow, or excellent: green). In a second tab, also shown in Figure 9, graphs provide information regarding the sample, including the porosity value along the slices, the quantity of pores in each visibility class, and a graph that shows the relationship between pore diameter and circularity.

The tool also allows the user to obtain a 3D view of the input slices, enabling them to interact and visualize the sample from different angles. Figure 10 illustrates this functionality.

Figure 10 – 3D view of a fracture sample and pore sample.
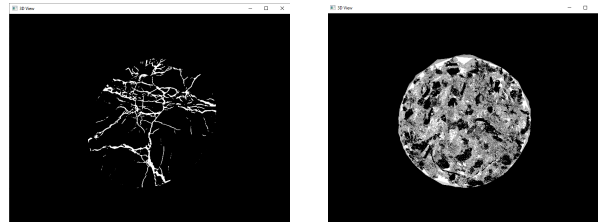
Source: The authors (2023).

To demonstrate the functionality and capabilities of the tool, we manually created an artificial microCT image containing fractures of various geometries. This allows us to evaluate how the tool performs specifically in fracture analysis.

The image shown in Figure 11 (a) contains 7 fractures labeled A to G, which were manually inserted to represent various fracture geometries. These fractures were designed to cover most of the parameters evaluated in the literature. Table 2 presents the results of some of the features evaluated by the tool.

Analyzing the results obtained, it is possible to perceive that the tool is able to provide answers that match the geometry of the fractures. However, depending on the orientation (horizontal/vertical) of the analyzed object, its length and width, in this case presented in pixels, may be inverted. Regarding the global analysis also provided by the tool, the presence of the 7 fractures was correctly identified, with the separation into 1 vertical, 1 horizontal and 5 inclined, with 28.5% of them being systematic (corresponding to 2 fractures, being A and E) and 71.4% non-systematic (corresponding to 5 fractures).

Figure 11 – Example of fractures and the response obtained in their processing. (a) artificial input image (b) output after image processing.

(a)   (b)
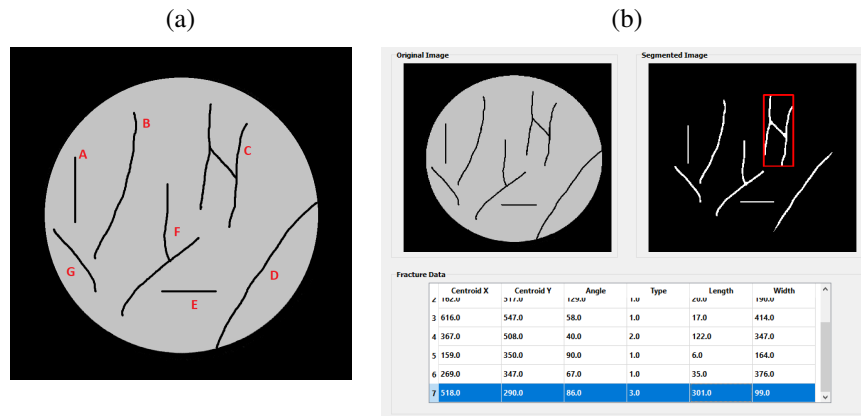
Source: The authors (2023).

Table 2 – Fracture geometry analysis.

Label	Angle	Type	Length	Width
A	90	1	6	164
B	67	1	35	376
C	86	3	301	99
D	58	1	17	414
E	179	1	137	6
F	39	2	122	347
G	129	1	20	190

6   CONCLUSIONS

A tool was created to analyze microtomography images and understand the behavior of porous and fractured carbonate rocks, which are commonly found in oil reservoirs. The tool calculates parameters that make it easier to locate and label extracted structures, compared to the manual procedures that are typically used.

Therefore, this study provides a valuable contribution to support reservoir modeling and characterization, by describing the petrophysical parameters of pores and fractures identified in processed microtomography images. The methodology applied here is essential in assisting the construction of geological models, which guide the development and management of an oil or gas field.

Acknowledgments

Authors' Contributions

L.S.B.: Conceptualization, Data Preparation, Data Analysis, Methodology, Implementation, Writing; G.D.A.: Data Interpretation, Supervision, Review; A.C.V.: Supervision, Funding Acquisition, Review; H.P.: Supervision, Writing, Review.

Conflict of Interest

The authors declare no conflict of interest.

References

ANSELMETTI, F.S.; LUTHI, S.; EBERLI, G.P. Quantitative Characterization of Carbonate Pore Systems by Digital Image Analysis. **American Association of Petroleum Geologists (AAPG) Bulletin**, American Association of Petroleum Geologists, v. 82, n. 10, p. 1815–1836, 1998.

ARCHIE, G.E. Classification of Carbonate Reservoir Rocks and Petrophysical Considerations. **American Association of Petroleum Geologists (AAPG) Bulletin**, American Association of Petroleum Geologists, v. 36, n. 2, p. 278–298, 1952.

BASAN, P.B.; LOWDEN, B.D.; WHATTLER, P.R.; ATTARD, J.J. Pore-Size Data in Petrophysics: A Perspective on the Measurement of Pore Geometry. **Geological Society, London, Special Publications**, Geological Society of London, v. 122, n. 1, p. 47–67, 1997.

BEUCHER, S.; MEYER, F. The Morphological Approach to Segmentation: The Watershed Transformation. **Mathematical Morphology in Image Processing**, CRC Press, p. 433–481, 2018.

BOMFIM, L.S.; PEDRINI, H. Characterization of Fracture Geometry with Computed Microtomography Rock Images. **XXIII Brazilian Symposium on GeoInformatics (GeoInfo)**, São José dos Campos, Brazil, p. 111–122, nov. 2022.

BULTREYS, T. **Estaillades Carbonate #2**. National Science Foundation: Digital Rocks Portal, 2016. http://www.digitalrocksportal.org/projects/58.

BULTREYS, T.; STAPPEN, J.; KOCK, T.; BOEVER, W.; BOONE, M.A.; HOOREBEKE, L.; CNUDDE, V. Investigating the Relative Permeability Behavior of Microporosity-Rich Carbonates and Tight Sandstones with Multiscale Pore Network Models. **Journal of Geophysical Research: Solid Earth**, Wiley Online Library, v. 121, n. 11, p. 7929–7945, 2016.

CNUDDE, V.; BOONE, M.N. High-resolution X-Ray Computed Tomography in Geosciences: A Review of the Current Technology and Applications. **Earth-Science Reviews**, Elsevier, v. 123, p. 1–17, 2013.

COUNCIL, National Research. **Rock Fractures and Fluid Flow: Contemporary Understanding and Applications**. Washington, DC, USA: National Academies Press, 1996. P. 568.

DENG, H.; FITTS, J.P.; PETERS, C.A. Quantifying Fracture Geometry with X-ray Tomography: Technique of Iterative Local Thresholding (TILT) for 3D Image Segmentation. **Computational Geosciences**, Springer, v. 20, n. 1, p. 231–244, 2016.

DONG, H.; FJELDSTAD, S.; ALBERTS, L.; ROTH, S.; BAKKE, S.; ØREN, P. Pore Network Modelling on Carbonate: A Comparative Study of Different Micro-CT Network Extraction Methods. **International Symposium of the Society of Core Analysts**, Abu Dhabi, United Arab Emirates, v. 29, p. 1–12, 2008.

ERTEKIN, T.; ABOU-KASSEM, J.H.; KING, G.R. **Basic Applied Reservoir Simulation**. Richardson, TX, USA: Society of Petroleum Engineers Richardson, 2001. v. 7.

GONZALEZ, R. C; WOODS, R.E. **Digital Image Processing**. Upper Saddle River, NJ, USA: Prentice Hall New Jersey, 2007.

HARDEBOL, N.J.; BERTOTTI, G. DigiFract: A Software and Data Model Implementation for Flexible Acquisition and Processing of Fracture Data from Outcrops. **Computers & Geosciences**, Elsevier, v. 54, p. 326–336, 2013.

HEALY, D.; RIZZO, R.E.; CORNWELL, D.G.; FARRELL, N.J.C.; WATKINS, H.; TIMMS, N.E.; GOMEZ-RIVAS, E.; SMITH, M. FracPaQ: A MATLAB Toolbox for the Quantification of Fracture Patterns. **Journal of Structural Geology**, Elsevier, v. 95, p. 1–16, 2017.

INTERSTATE TECHNOLOGY AND REGULATORY COUNCIL (ITRC). **Characterization and Remediation in Fractured Rocks**. Washington, DC, USA: Environmental Council of the States, 2020. https://fracturedrx-1.itrcweb.org/3-hydrology-fluid-flow/.

JING, L.; STEPHANSSON, O. **Fundamentals of Discrete Element Methods for Rock Engineering: Theory and Applications**. Amsterdam, The Netherlands: Elsevier, 2007. v. 85.

LI, M.; MAGSIPOC, E.; ABDELAZIZ, A.; HA, J.; PETERSON, K.; GRASSELLI, G. Mapping Fracture Complexity of Fractured Shale in Laboratory: Three-Dimensional Reconstruction from Serial-Section Images. **Rock Mechanics and Rock Engineering**, Springer, v. 55, n. 5, p. 2937–2948, 2022.

LI, W.; FRASH, L.P.; WELCH, N.J.; CAREY, W.J.; MENG, M.; WIGAND, M. Stress-Dependent Fracture Permeability Measurements and Implications for Shale Gas Production. **Fuel**, Elsevier, v. 290, p. 119984, 2021.

LUCIA, F.J.; KERANS, C.; JENNINGS, J.W. Carbonate Reservoir Characterization. **Journal of Petroleum Technology**, OnePetro, v. 55, n. 6, p. 70–72, 2003.

MACDONALD, D.A.; BARTKOWIAK, T.; MENDAK, M.; STEMP, W.J.; KEY, A.; DE LA TORRE, I.; WIECZOROWSKI, M. Revisiting Lithic Edge Characterization with MicroCT: Multiscale Study of Edge Curvature, Re-Entrant Features, and Profile Geometry on Olduvai Gorge Quartzite Flakes. **Archaeological and Anthropological Sciences**, Springer, v. 14, n. 2, p. 1–20, 2022.

MORAES, P.C.X. **Determinação de Propriedades Petrofísicas e Geológicas utilizando uma Técnica de Análise Digital de Rochas**. 2018. Diss. (Mestrado) – Faculdade de Engenharia Mecânica e Instituto de Geociências, Universidade Estadual de Campinas, Campinas-SP.

OPENCV. **Open Source Computer Vision Library**. OpenCV Team: GitHub, Inc., 2015. https://github.com/opencv/opencv.

ORTEGA, O.; MARRETT, R. Prediction of Macrofracture Properties using Microfracture Information, Mesaverde Group Sandstones, San Juan Basin, New Mexico. **Journal of Structural Geology**, Elsevier, v. 22, n. 5, p. 571–588, 2000.

OTSU, N. A Threshold Selection Method from Gray-Level Histograms. **IEEE Transactions on Systems, Man, and Cybernetics**, IEEE, v. 9, n. 1, p. 62–66, 1979.

PEDRINI, H. Multiresolution Terrain Modeling Based on Triangulated Irregular Networks. **Revista Brasileira de Geociências**, v. 31, n. 2, p. 117–122, jun. 2001.

PEDRINI, H.; SCHWARTZ, W.R. **Análise de Imagens Digitais: Princípios, Algoritmos e Aplicações**. São Paulo, SP, Brazil: Editora Thomson Learning, 2007.

PLASIS, A. **Concrete Cracking**. Stellenbosch, South Africa: Stellenbosch University, 2014. http://blogs.sun.ac.za/ctscanner/concrete-cracking/.

PURSWANI, P.; KARPYN, Z.T.; ENAB, K.; XUE, Y.; HUANG, X. Evaluation of Image Segmentation Techniques for Image-based Rock Property Estimation. **Journal of Petroleum Science and Engineering**, Elsevier, v. 195, p. 107890, 2020.

RAMANDI, H.L.; IRTZA, S.; SIROJAN, T.; NAMAN, A.; MATHEW, R.; SETHU, V.; ROSHAN, H. FracDetect: A Novel Algorithm for 3D Fracture Detection in Digital Fractured Rocks. **Journal of Hydrology**, Elsevier, v. 607, p. 127482, 2022.

SANTOS, A.; SCANAVINI, H.F.A.; PEDRINI, H.; SCHIOZER, D.J.; MUNERATO, F.P.; BARRETO, C.E.A.G. An Artificial Intelligence Method for Improving Upscaling in Complex Reservoirs. **Journal of Petroleum Science and Engineering**, v. 211, p. 110071, 2022.

SCHWARTZ, W.R.; PEDRINI. Textured Image Segmentation Based on Spatial Dependence Using a Markov Random Field Model. **IEEE International Conference on Image Processing**, Atlanta, GA, USA, v. 1, p. 2449–2452, out. 2006.

SHAFLOOT, T.A.; KIM, T.W.; KOVSCEK, A.R. Investigating Fracture Propagation Characteristics in Shale Using sc-CO2 and Water with the Aid of X-ray Computed Tomography. **Journal of Natural Gas Science and Engineering**, v. 92, p. 103736, 2021.

SINGHAL, B.; GUPTA, R. **Applied Hydrogeology of Fractured Rocks**. New York, NY, USA: Springer Science & Business Media, 2010. P. 408.

SOK, R.M.; KNACKSTEDT, M.A.; VARSLOT, T.; GHOUS, A.; LATHAM, S.; SHEPPARD, A.P. Pore Scale Characterization of Carbonates at Multiple Scales: Integration of Micro-CT, BSEM, and FIBSEM. **Petrophysics**, Society of Petrophysicists e Well-Log Analysts, v. 51, n. 6, 2010.

TANG, Y.B.; LI, M.; LI, X.F. Connectivity, Formation Factor and Permeability of 2D Fracture Network. **Physica A: Statistical Mechanics and its Applications**, Elsevier, v. 483, p. 319–329, 2017.

VAN DER WALT, S.; SCHÖNBERGER, J.L.; NUNEZ-IGLESIAS, J.; BOULOGNE, F.; WARNER, J.D.; YAGER, N.; GOUILLART, E.; YU, T. Scikit-Image: Image Processing in Python. **PeerJ**, PeerJ Inc., v. 2, e453, 2014.

VIRTANEN, P.; GOMMERS, R.; OLIPHANT, T.E.; HABERLAND, M.; REDDY, T.; COURNAPEAU, D.; BUROVSKI, E.; PETERSON, P.; WECKESSER, W.; BRIGHT, J.; WALT, S.J. van der; BRETT, M.; WILSON, J.; JARROD, K.; MAYOROV, N.; NELSON, A.R.J.; JONES, E.; KERN, R.; LARSON, E.; CAREY, C.J.; POLAT, I.; FENG, Y; MOORE, E.W.; VAN DER PLAS, J.; LAXALDE, D.; PERKTOLD, J.; CIMRMAN, R.; HENRIKSEN, I.; QUINTERO, E.A.; HARRIS, C.R.; ARCHIBALD, A.M.; RIBEIRO, A.H.; PEDREGOSA, F.; VAN MULBREGT, P. SciPy 1.0: Fundamental Algorithms for Scientific Computing in Python. **Nature Methods**, v. 17, p. 261–272, 2020.

WIGGINS, R.H.; DAVIDSON, H.C.; HARNSBERGER, H.R.; LAUMAN, J.R.; GOEDE, P.A. Image File Formats: Past, Present, and Future. **Radiographics**, Radiological Society of North America, v. 21, n. 3, p. 789–798, 2001.

XIONG, F.; JIANG, Q.; XU, C. Fast Equivalent Micro-Scale Pipe Network Representation of Rock Fractures Obtained by Computed Tomography for Fluid Flow Simulations. **Rock Mechanics and Rock Engineering**, Springer, v. 54, n. 2, p. 937–953, 2021.

YANG, B.; WANG, H.; WANG, B.; SHEN, Z.; ZHENG, Y.; JIA, Z.; YAN, W. Digital Quantification of Fracture in Full-Scale Rock Using Micro-CT Images: A Fracturing Experiment With N2 and CO2. **Journal of Petroleum Science and Engineering**, v. 196, p. 107682, 2021.

ZHU, W.; KHIREVICH, S.; PATZEK, T.W. Impact of Fracture Geometry and Topology on the Connectivity and Flow Properties of Stochastic Fracture Networks. **Water Resources Research**, Wiley Online Library, v. 57, n. 7, p. 1–15, 2021.

Main Author's Biography

Letícia da Silva Bomfim is currently a Ph.D. student in Computer Science in the Institute of Computing of the University of Campinas (UNICAMP), Campinas-SP, Brazil. She received her B.Sc. in Computer Science from the State University of Santa Cruz (UESC), Ilhéus-BA, Brazil. She received her M.Sc. in Computer Science from the University of Campinas (UNICAMP), Campinas-SP, Brazil. Her main research interests include image processing, machine learning, scientific visualization.